Evidence for Breaking Domain−Domain Functional Communication in a Synthetase−tRNA Complex†

Rebecca W. Alexander and Paul Schimmel*

The Skaggs Institute for Chemical Biology, The Scripps Research Institute, 10550 North Torrey Pines Road, La Jolla, California 92037

Received August 19, 1999; Revised Manuscript Received October 12, 1999

ABSTRACT: We report here evidence for mutations that break domain−domain functional communication in a synthetase−tRNA complex. Each synthetase is roughly divided into two major domains that are paralleled by the two arms of the L-shaped tRNA structure. The active-site-containing domain interacts with the acceptor arm of the tRNA. The second domain frequently interacts with the anticodon-containing arm. By an induced-fit mechanism, contacts with the anticodon can activate formation of a robust transition state at a site over 70 Å away. This induced-fit-based activation is thought to occur through domain−domain signaling and is seen by the enhancement of aminoacylation of the anticodon-containing full tRNA versus a substrate based on the acceptor arm alone. Here we describe a rationally designed mutant methionyl-tRNA synthetase containing two point substitutions at sites that potentially link an anticodon-binding motif to the catalytic domain. The double mutation had no effect on interactions with either the isolated acceptor arm or the anticodon stem-loop. In contrast to interactions with the separate pieces, the mutant enzyme was severely impaired for binding the native tRNA and lost much of its ability to enhance the rate of charging of the full tRNA over that of a substrate based on the acceptor arm alone. We propose that these residues are part of a network for facilitating domain−domain communication for formation of an active synthetase−tRNA complex by induced fit.

Aminoacyl-tRNA synthetases (aaRSs)[1] catalyze the attachment of amino acids to their cognate tRNA molecules, thereby establishing the rules of the genetic code. The 20 aaRSs can be divided into two classes of 10 enzymes, each based on sequence and structural similarities of their catalytic cores (*1*−*3*). The class I family is defined by an active site Rossmann nucleotide binding fold containing a dodecapeptide signature sequence ending in HIGH as well as a second motif having the sequence KMSKS (*1*, *2*, *4*, *5*). In addition to the class-defining catalytic domain, many aaRSs also contain a second major domain that is idiosyncratic to each synthetase. The two-domain structural organization parallels the arrangement of the two arms of the L-shaped tRNA molecule. These arms contain the 3′-acceptor end and the anticodon, respectively. In the synthetase−tRNA complex, the two arms of the tRNA make contacts with, respectively, the two major domains of the enzyme.

In some cases, the anticodon portion of the tRNA molecule makes no contact with the enzyme. Examples include AlaRS and SerRS (*3*, *6*, *7*). In contrast, other aaRSs such as MetRS make critical contacts with their cognate tRNA anticodons (*8*−*11*). Methionyl-tRNA synthetase is a well-studied example of the two-domain organization of a class I aaRS, with the catalytic domain contained in the N-terminal half (*12*). Functional contacts with the $tRNA^{Met}$ CAU anticodon are made by the predominantly α-helical C-terminal domain of the protein, where a loop containing a highly conserved Trp461 (W461) plays an important role (*13*−*15*). Although the $tRNA^{Met}$ CAU anticodon is a strong determinant for aminoacylation by MetRS (*8*, *15*−*17*), substitution of the N73 discriminator base or a G72G73 substitution in the acceptor stem severely reduces aminoacylation efficiency (*18*). Indeed, small RNA substrates based on only the acceptor stem of $tRNA^{Met}$ are methionylated at a low rate in a sequence-dependent way (*19*, *20*). Interestingly, even though the anticodon arm in isolation binds to the C-terminal domain of MetRS (*15*, *21*), no enhancement of microhelix aminoacylation occurs upon its addition (*22*). Thus, efficient catalysis requires covalent continuity of the tRNA structure.

Significantly, functions specific to the catalytic core of the enzyme do not require an intact anticodon-binding domain. For example, deletion of 11 amino acids surrounding W461 in the anticodon-binding domain produces a mutant MetRS deficient in tRNA aminoacylation and anticodon binding, but nonetheless competent for methionyl-adenylate synthesis and microhelix aminoacylation (*23*). These results point to the necessity for long-range communication between the anticodon-binding domain and the catalytic site. This communication may be at the heart of the induced-fit mechanism of synthetase−tRNA interaction described earlier for this system (*24*). Induced fit may trigger a distortion of the 3′-terminus of the tRNA molecule to properly present

† Supported by Grant GM15539 from the National Institutes of Health. R.W.A. was an NIH postdoctoral fellow.

* To whom correspondence should be addressed. Phone: (858) 784-8972. Fax: (858) 784-8990. E-mail: schimmel@scripps.edu.

[1] Abbreviations: aaRS, aminoacyl-tRNA synthetase; MetRS, methionyl-tRNA synthetase; AlaRS, alanyl-tRNA synthetase; SerRS, seryl-tRNA synthetase; GlnRS, glutaminyl-tRNA synthetase; IPTG, isopropyl-1-thio-β-D-galactopyranoside; Ni-NTA, N^{2+}-nitrilotriacetic acid; EDTA, ethylenediaminetetraacetic acid; Hepes, *N*-(2-hydroxyethyl)piperazine-*N*′-2-ethanesulfonic acid; BSA, bovine serum albumin.

10.1021/bi991948c CCC: $18.00
Published on Web 11/10/1999

the acceptor end to the active site of the enzyme (*22*, *25*, *26*).

To evaluate how the protein architecture contributes to domain−domain signaling and induced fit, we mutated a site in the anticodon-binding domain and in a helix joining that domain to the catalytic core of the enzyme. These sites were chosen because a structural model suggested that, while well-separated in the sequence, they were close enough in space to link together the two parts of the protein (*12*). In addition, one of the sites was reported earlier to be in the structural unit that is particularly sensitive to induced-fit dependent interactions (*10*, *27*). Our results show that these residues contact neither the anticodon stem-loop nor the acceptor stem. The lack of a direct contact with tRNA is consistent with a model of the complex that shows these residues are not at the enzyme−tRNA interface (*26*). Yet, together these residues are shown here to contribute significantly to the stability of the synthetase−tRNA complex and to the catalytic efficiency of aminoacylation. We propose that these sites may be important for induced-fit-directed binding of the active conformation of the two domains of methionine-specific tRNA.

MATERIALS AND METHODS

Construction and Purification of MetRS Variants. For ease of purification, the highly active monomeric N-terminal fragment of 547 amino acids of *Escherichia coli* MetRS was used for all investigations reported here. All MetRS proteins studied here incorporated a 6-His tag at their N-terminus. (We showed that tagged and untagged enzyme had the same value of k_{cat}/K_M for $tRNA^{fMet}$ in the aminoacylation assay.) Amino acid substitutions were introduced into the gene (6H MRS 547) for MetRS [that was cloned into pBluesript(+) (*22*)] using mutagenic primers and the polymerase chain reaction. The resulting variant plasmids were confirmed by sequencing and transformed into *E. coli* strain JM109 (*28*) for protein overexpression and purification. After induction of protein expression with 1 mM IPTG, cells were harvested at mid-log phase. Proteins were purified by Ni−NTA agarose affinity chromatography according to the manufacturer's protocol [Qiagen (Chatworth, CA)]. Protein concentrations were determined in a Bradford assay using Bio-Rad protein reagent and a standard curve of BSA (*29*).

Synthesis of RNA Substrates. The $tRNA_2^{fMet}$ substrate was overproduced in vivo as previously described (*30*), purified on a 16% native polyacrylamide gel, and passively eluted from the gel in 0.5 M NH_4OAc (pH 5.4) and 1 mM EDTA. $Microhelix^{fMet}$ and hairpin helices corresponding to the anticodon stem and loop of $tRNA^{fMet}$ were chemically synthesized on a Pharmacia GeneAssembler Special using N-phenoxyacetyl-protected 2′-*tert*-butyl-dimethylsilyl ribonucleoside 3′-cyanoethyl phosphoramidites from ChemGenes (Waltham, MA). Deprotection and gel purification were carried out as described (*22*). The anticodon stem-loop hairpin based on $tRNA^{fMet}$ had the sequence 5′-GUCGGGCU-**CAU**AACCCGAC-3′, with the wild-type CAU anticodon indicated in bold. A GAU-containing hairpin was also constructed with a C to G substitution at the first anticodon position.

Aminoacylation Assays. Aminoacylation of $tRNA^{fMet}$ or $microhelix^{fMet}$ was carried out at 25 °C in 20 mM Hepes (pH 7.5), 100 μM Na_2EDTA, 150 mM NH_4Cl, 4 mM ATP, 10 mM $MgCl_2$, 100 μM methionine, [^{35}S]methionine [NEN-DuPont (50 mCi/mL; 1 Ci = 37 GBq)], and varying concentrations of wild-type or mutant MetRS. RNAs were annealed before use by heating to 80 °C followed by slow cooling to room temperature in the presence of 1 mM $MgCl_2$. The $tRNA^{fMet}$ was typically assayed at a concentration of 5 μM, while $micro^{fMet}$ was assayed at 100−200 μM. MetRS variants were used at concentrations of 50 nM or 10 μM for aminoacylation of $tRNA^{fMet}$ or $Micro^{fMet}$, respectively. For kinetic characterizations, enzyme concentrations were 50 nM for wild-type, N387A and N452A MetRS, and 500 nM for N387A/N452A MetRS. For these experiments, $tRNA^{fMet}$ concentrations were 0.5−20 μM for the wild-type enzyme, 1−50 μM for N387A, 1−75 μM for the N452A enzyme, and 1−100 μM for N387A/N452A MetRS. Reaction aliquots (5 μL) were quenched by spotting on Whatman filters soaked in 5% trichloroacetic acid and 1 mM methionine. The filters were washed for five 10 min periods in ice-cold 5% trichloroacetic acid/1 mM methionine before liquid scintillation counting.

ATP−PP_i Exchange Assay. The formation of methionyl-adenylate was monitored in the methionine-dependent ATP-pyrophosphate exchange reaction according to (*31*). Reactions were carried out at 25 °C in 100 mM Tris-HCl (pH 7.5), 10 mM KF, 7 mM 2-mercaptoethanol, 5 mM $MgCl_2$, 2 mM ATP, 100 μg/mL BSA, 200 μM methionine, 2 mM $NaPP_i$, and [^{32}P] $NaPP_i$ (NEN-DuPont). Wild-type and mutant MetRS enzymes were assayed at 50 nM. Reaction aliquots (10 μL) were quenched into microfuge tubes containing 0.2 M PP_i, 7% $HClO_4$, and 3% charcoal and mixed thoroughly. The charcoal was washed three times with 10 mM PP_i and 0.5% $HClO_4$, and the tubes were spun briefly after each wash to recover the charcoal, which was then analyzed by scintillation counting.

Fluorescence Quenching. Quenching of intrinsic MetRS tryptophan fluorescence in the presence of $tRNA^{fMet}$ was carried out essentially according to Blanquet and co-workers (*27*, *32*). Fluorescence measurements were made using a Perkin-Elmer LS 50 Luminescence Spectrometer (Perkin-Elmer Ltd, Beaconsfield, Buckinghamshire, England). Samples were stirred continuously at room temperature. Wild-type or N387A/N452A MetRS (0.2 μM) was excited at 295 nm, and fluorescence emission was detected at 328 nm in 20 mM Tris-HCl (pH 7.6), 10 mM 2-mercaptoethanol, 8 mM $MgCl_2$, and 0.1 mM EDTA. Intrinsic fluorescence was quenched by titration of $tRNA^{fMet}$ in 5 μL aliquots in the same buffer, with each addition increasing the tRNA concentration by 0.2 μM. Correction for dilution and inner-filter effects was accomplished by subtracting the fluorescence quench obtained by titration with an equivalent solution of $tRNA^{fMet}$ digested with RNase [DNase-free; Boehringer Mannheim Biochemicals (Indianapolis, IN)] at a concentration of 40 units/mL.

RESULTS

Rationale for Mutations That Could Affect Domain−Domain Signaling. E. coli methionyl-tRNA synthetase is a dimer of identical 676 amino acid polypeptides (*33*). A C-terminal deletion removes the region required for dimerization and results in an N-terminal fragment of 547 amino

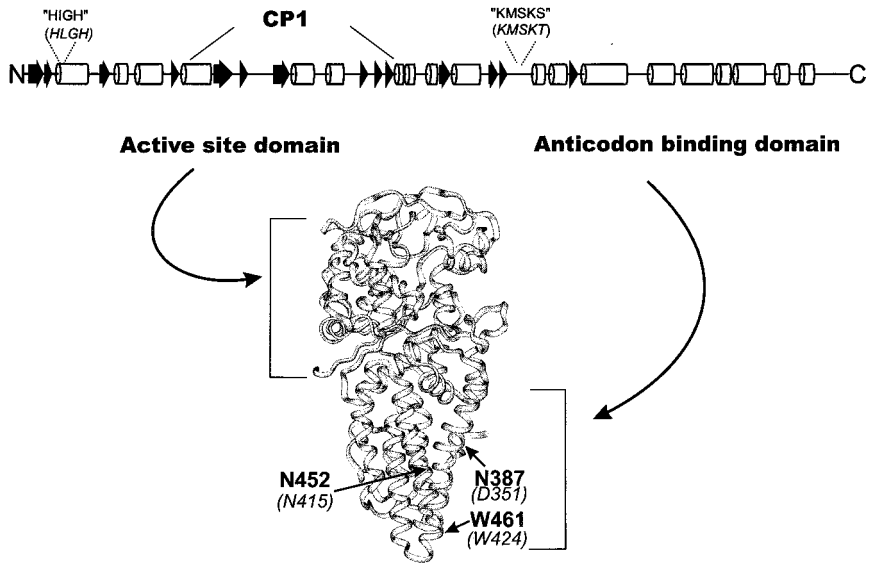

FIGURE 1: Secondary structure diagram (top) and crystal structure [bottom (*36*)] of *T. thermophilus* MetRS. In the secondary structure diagram, helices are designated with cylinders and β-strands are indicated with arrows. Numbering is given for the *E. coli* enzyme, with corresponding residues for the *T. thermophilus* enzyme in italics.

acids that is monomeric and has almost the same catalytic activity as the native dimer (*34*). The gene for this fragment also complements a null allele that removes the gene for methionyl-tRNA synthetase from the *E. coli* chromosome (*35*). To study domain−domain signaling within the catalytic unit itself and to isolate this signaling from potential effects of the dimer interface, the monomeric N-terminal fragment of MetRS was used in all investigations reported here. The robust in vitro and in vivo activity of this fragment provided additional justification for this strategy.

Within the monomeric 547 amino acid fragment, the N-terminal approximately 350 amino acids is organized into a Rossmann nucleotide binding fold that is characteristic of all class I enzymes (*12*). The alternating β-strands and α-helices of this fold form the active site for adenylate synthesis and for attachment of methionine to the 3′-end of $tRNA^{Met}$. A linker joins the C-terminal end of the active-site-containing domain to the C-terminal domain that is largely made up of α-helices (Figure 1). In particular, a critical helix for anticodon interactions extends from K439 to A459. A loop sandwiched between this helix and a second helix that starts at A471 contains P460, W461, and K465, each of which is essential for anticodon interactions (*10*). We sought to identify positions in the structure of MetRS that would influence the conformation and position of this loop, on one hand, and communicate with the N-terminal active-site-containing domain on the other.

For this purpose, we focused on the highly conserved N452, because this asparagine is within the aforementioned helix and had been shown previously to contribute to anticodon recognition, possibly by affecting the orientation of one or more members of the critical P460, W461, and K465 triad (*10*, *27*). With the intact tRNA, the interactions with this part of MetRS appear to be induced-fit dependent (*24*). The rationale was that N452 might be a place where another conserved residue would potentially interact and link the helix back to the catalytic domain. In this connection, N452 is close in space to the conserved N387, which itself is in a helix that joins the C-terminal structural unit to the active-site domain (Figure 1). Although an interaction between these residues has not been established, in the structure of the homologous *T. thermophilus* enzyme, these two residues are sufficiently close (~7 Å) that their functional groups could provide at least some of the basis for communication between the two domains of MetRS (*36*). Thus, the functional side-chain atoms of N387 and N452 were replaced with a methyl group by making single and double alanine replacements within MetRS.

Expression and Purification of MetRS Variants. Wild-type, N387A, N452A, and N387A/N452A MetRS were overexpressed from a pBluescript(+) plasmid that encoded each of the genes for the respective proteins behind an inducible *lac* promoter. Although the proteins were expressed in *E. coli* strain JM109, which harbors the gene for the wild-type native MetRS on the chromosome, the $(His)_6$-tag on the variant proteins afforded an easy way to isolate them away from the native enzyme. Enzymes purified by NiNTA-affinity chromatography were confirmed to be homogeneous by SDS−PAGE under conditions where any contamination of the plasmid-encoded proteins (547 amino acid monomer) by chromosome-encoded wild-type enzyme (dimer of identical 676 amino acid polypeptides) would have been evident. Each MetRS variant was purified with a yield approximating that of the plasmid-encoded wild-type MetRS monomer. This observation showed that the N387A, N452A, and N387A/N452A substitutions cause no structural instabilities that would lead to protein degradation within the cell.

$tRNA^{fMet}$ Binding Is Significantly Perturbed by the Double N387A/N452A Mutation. To determine the effect of the mutations in the C-terminal domain of MetRS on binding of $tRNA^{fMet}$, we used intrinsic tryptophan fluorescence in the absence and presence of tRNA to measure apparent dissociation constants for the MetRS−$tRNA^{fMet}$ complex. A hyperbolic fit of the relative quenching of fluorescence upon titration with tRNA demonstrated that wild-type MetRS bound $tRNA^{fMet}$ with an apparent K_d of 0.41 ± 0.03 μM at pH 7.6, 25 °C. In contrast, addition of $tRNA^{fMet}$ to the N387A/N452A enzyme produced no binding-dependent change in fluorescence, indicating negligible complex formation under the conditions used (data not shown).

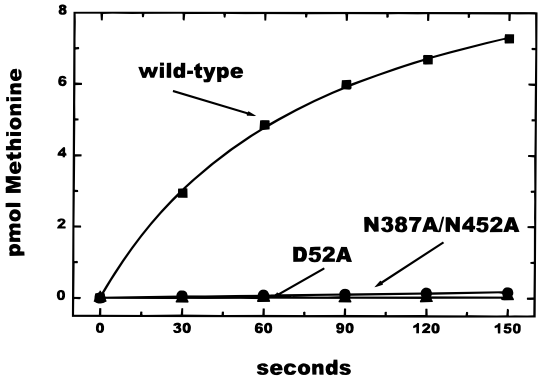

FIGURE 2: Aminoacylation of $tRNA^{fMet}$ with MetRS variants at pH 7.5, 25 °C. Wild-type MetRS, D52A, and N387A/N452A mutant enzymes were assayed at 50 nM in the presence of 2 μM $tRNA^{fMet}$ and 100 μM methionine. The efficiency of aminoacylation by the double mutant N387A/N452A is significantly decreased relative to the wild-type enzyme.

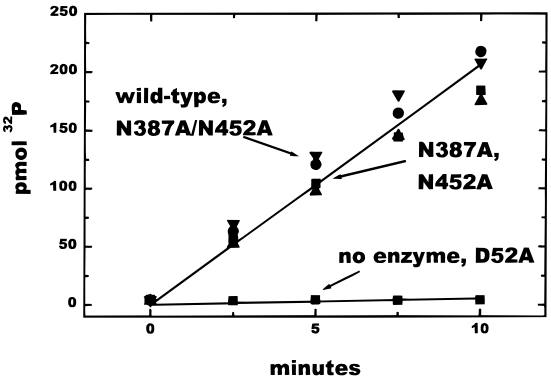

FIGURE 3: Methionyl-adenylate formation of MetRS variants. Wild-type MetRS and N387A, N452A, N387A/N452A, and D52A mutant enzymes were assayed at 50 nM enzyme and 200 μM methionine at 25 °C in an ATP−PP_i exchange assay.

Our results with the N387A/N452A mutant enzyme are compatible with fluorescence titrations of $tRNA^{fMet}$ with the N387 and N452 mutant proteins (*9*, *27*). These studies reported a decrease in affinity of the mutant proteins for $tRNA^{fMet}$. This decrease was attributed, however, to an effect on MetRS interactions with the anticodon. To check further the validity of our own studies with the double mutant, we used a different assay to study directly the interaction of the anticodon with the wild-type and mutant enzymes. These studies showed that the N387A/N452A double mutation has no effect on anticodon interactions (see below).

Loss of tRNA Aminoacylation Enhancement by Double Mutant. Having established that tRNA-binding contacts were significantly perturbed by the N387A/N452A double sustitution in MetRS, we investigated the effect of the N387, N452, and N387/N452 mutations on the aminoacylation of $tRNA^{fMet}$. The rate of aminoacylation of the full-length $tRNA^{fMet}$ substrate by N387A/N452A MetRS was reduced more than 30-fold relative to the wild-type enzyme (Figure 2). To determine whether the large reduction in the rate of aminoacylation was caused primarily by the N387A or the N452A substitution, we studied each of the single-substituted enzymes. Each of the proteins bearing a single mutation had a catalytic efficiency (k_{cat}/K_M) that was decreased less than 3-fold. Thus, the effect of either of the single substitutions was to make the activity of the enzyme especially vulnerable to the second amino acid replacement. This behavior is consistent with N387 and N452 jointly forming part of the connection that links the anticodon-binding domain to the active site.

Activation of Methionine by Variant Enzymes. Because N387 and N452 were potentially linked back to the catalytic domain, we were aware that alanine replacements of these residues might perturb the tRNA-dependent step of aminoacylation because of an effect on amino acid activation. Were amino acid activation to be directly affected by the N387A and N452A substitutions, the analysis of the tRNA-dependent part of domain−domain signaling would be difficult to interpret. To determine whether amino acid substitutions outside the active site of the enzyme had any effect on the methionine activation function of the variants, methionyl-adenylate formation was measured in the classical ATP−PP_i exchange assay. According to this assay, the rate of methionyl-adenylate formation was identical for N387A, N452A, N387A/N452A, and wild-type enzymes (Figure 3). As a negative control, we also prepared a D52A variant of MetRS. The D52A replacement is known to disrupt binding of methionine and thereby inhibit synthesis of methionyl adenylate (*37*). We confirmed that the D52A variant is significantly inhibited in methionine activation relative to the wild-type enzyme. Thus, the N387A, N452A, and N387A/N452A mutations have no effect on the active site, in the absence of tRNA.

Effect of N387A/N452A Mutation on Charging of Microhelix^{fmet}. The effect of the N387/N452 mutation on charging of $tRNA^{Met}$ could be due to domain−domain signaling that specifically perturbs the orientation and binding of the acceptor stem per se to the active-site region, in the absence of any contribution from anticodon interactions. With this in mind, we studied the effect of these substitutions on the aminoacylation of an RNA substrate that interacts solely with the N-terminal catalytic domain. We chose $microhelix^{fMet}$ because it is charged specifically by methionyl-tRNA synthetase and because it lacks the anticodon-containing domain of $tRNA^{fMet}$ (*19*, *20*) (Figure 4). The double mutant N387A/N452A MetRS aminoacylated a $microhelix^{fMet}$ with an efficiency nearly identical to that of the wild-type enzyme (Figure 5). The N387A and N452A enzymes also aminoacylate $microhelix^{fMet}$ with no loss in efficiency relative to the wild-type enzyme (not shown). Thus, the effect of the N387/N452 double substitution on charging of $tRNA^{fMet}$ requires interactions outside of the microhelix. These interactions presumably require the anticodon-containing domain of $tRNA^{fMet}$, which is missing in the microhelix substrate.

No Effect of N387A/N452A Substitution on Binding of Anticodon Stem-Loop. The results obtained to this point showed that the N387A/N452A substitution did not perturb the active site either in the absence of an RNA substrate or in the presence of a microhelix substrate. The full-length tRNA molecule differs from the microhelix in that the former has the second, anticodon-containing domain. Because our interests focused on the possibility of signaling from the anticodon to the active site about 75 Å away, we wanted to investigate further the possibility that anticodon-binding interactions were perturbed by the N387A/N452A double substitution. To investigate this point, we prepared an RNA hairpin that recreated the anticodon stem-loop of $tRNA^{fMet}$ (Figure 4). This stem-loop structure is known to be a

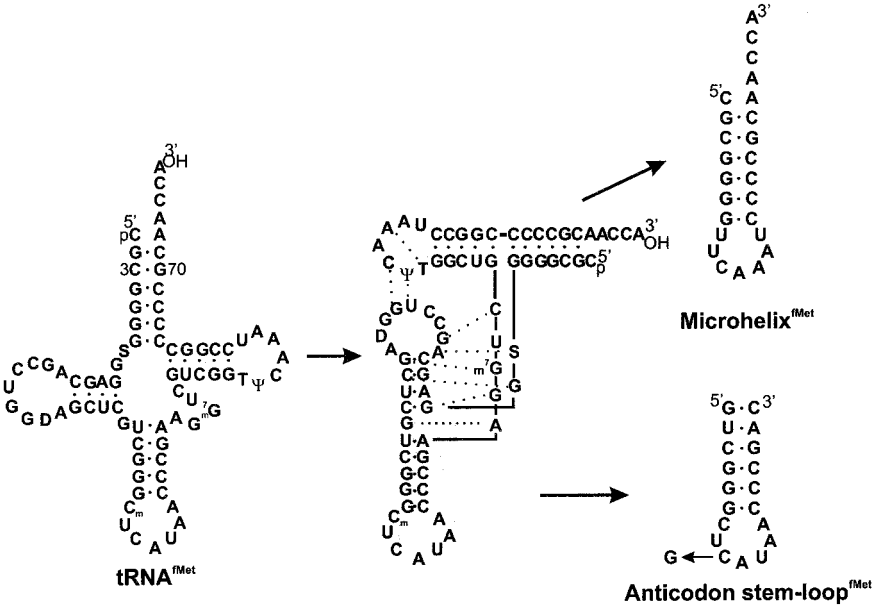

FIGURE 4: Sequences of tRNA^{fMet} and microhelix^{fMet} substrates and of the anticodon stem-loop^{fMet} hairpin. The cloverleaf sequence of tRNA^{fMet} (left) folds up into an L-shaped molecule in solution (center). Shading in the acceptor stem and TΨC loop indicate the portions of tRNA^{fMet} recapitulated in the microhelix^{fMet} substrate (top right) while the shading in the anticodon stem and loop indicates the sequence of the anticodon hairpin oligonucleotide (bottom right), closed by addition to the 3′-end of a C to form a G−C pair.

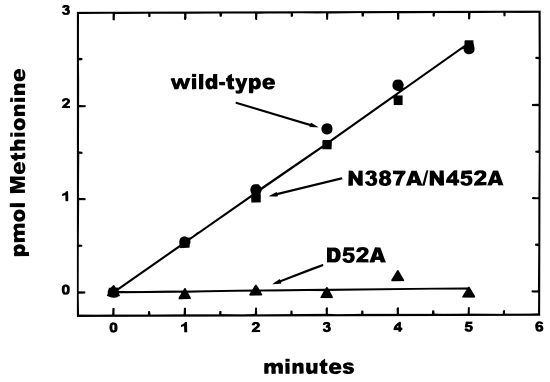

FIGURE 5: Aminoacylation of micohelix^{fMet} with enzyme variants at pH 7.5, 25 °C. Wild-type, D52A, and N387A/N452A MetRS were assayed at 10 μM in the presence of 200 μM microhelix^{fMet} and 100 μM methionine. The double mutant N387A/N452A aminoacylates the microhelix substrate at the same rate as the wild-type enzyme.

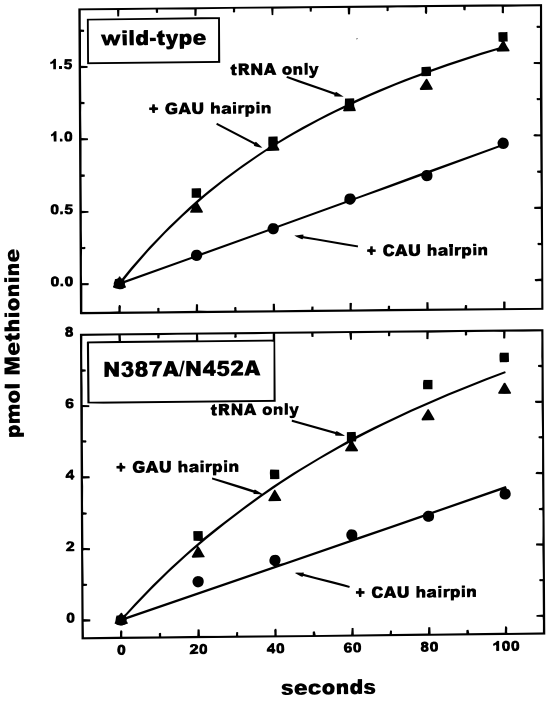

FIGURE 6: Inhibition of tRNA^{fMet} aminoacylation by CAU-containing anticodon stem-loop hairpin. Wild-type MetRS and the N387A/N452A mutant enzyme were assayed at pH 7.5, 25 °C, in the absence of any added oligonucleotide or in the presence of 140 μM CAU- or GAU-containing anticodon stem-loop hairpin. Wild-type MetRS was assayed at 30 nM in the presence of 0.7 μM tRNA^{fMet} (top); N387A/N452A MetRS was assayed at 0.5 μM in the presence of 7 μM tRNA^{fMet} (bottom). The CAU-containing hairpin inhibits tRNA aminoacylation while the GAU-containing hairpin has no effect on aminoacylation.

competitive inhibitor of aminoacylation of tRNA^{fMet} (*15*). We confirmed this inhibition with the wild-type enzyme and then went on to find that the N387A/N452A MetRS was inhibited by the anticodon stem-loop hairpin with a similar K_i as that of the native protein (K_i for aminoacylation by wild-type enzyme, 86 μM; K_i for aminoacylation by N387A/N452A enzyme, 134 μM). As a control, we showed that a CAU → GAU change of the anticodon triplet resulted in a hairpin oligonucleotide that no longer caused inhibition, as shown in Figure 6. Thus, the inhibition observed with the CAU-containing hairpin oligonucleotide is sequence specific. These results, together with the lack of an effect of the double substitution on the aminoacylation of the microhelix^{fMet} substrate, collectively demonstrate that the mutations do not affect any protein−RNA binding contact.

Kinetic Parameters for Aminoacylation of Wild-Type versus N387A/N452A Mutant Enzyme. The sharp decrease in the efficiency of charging (k_{cat}/K_m) of tRNA^{fMet} by the N387A/N452A enzyme is due at least in part to a weakening of the synthetase−tRNA complex. We were interested in determining in more detail the nature of the change in kinetic parameters for aminoacylation caused by the mutant enzyme. We measured the concentration dependence of the rate of aminoacylation with respect to tRNA over a range of 0.5−

Table 1: Kinetic Constants for Aminoacylation of tRNA^{f}Met by Wild-Type and Mutant MetRS[a]

MetRS variant	K_d (μM) (tRNA^{f}Met)	K_M (μM) (tRNA^{f}Met)	k_{cat} (s^{-1})	k_{cat}/K_M ($M^{-1}s^{-1}$)	relative efficiency
wild-type	0.41 ± 0.03	7 ± 1	1.11 ± 0.09	1.4×10^5	1
N387A/N452A	NM	68 ± 8	0.33 ± 0.02	4800	0.03

[a] Each value is determined from a hyperbolic fit of two independent data sets. NM, not measurable.

20 μM for the wild-type and 1−100 μM for the N387A/N452A enzyme. For the mutant enzyme, the K_m parameter was raised almost 10-fold, while k_{cat} was reduced more than 3-fold (Table 1). Together, the two parameters alter k_{cat}/K_m by more than 30-fold.

The K_m of 7 μM for the wild-type enzyme is nearly 20-fold higher than the K_d measured in our tRNA-binding assay (Table 1). The large discrepancy between the kinetic K_m and the thermodynamic K_d suggests that kinetic steps that occur after the initial binding interaction affect the K_m parameter and that these steps compete kinetically with the dissociation of the tRNA from the enzyme. Thus, the N387/N452-dependent linkage between the anticodon-binding domain and the active site establishes a complex (k_{cat} and K_m) kinetic communication between the anticodon-containing domain and the active site.

DISCUSSION

A comparison of the crystal structures of *E. coli* MetRS and GlnRS reveals significant similarities between the two enzymes despite an overall lack of sequence identity (*26*). The structure of the tRNA^{Gln}−GlnRS complex has been particularly informative regarding specific RNA−protein contacts (*25*, *38*, *39*), and provides a rationale for many of the effects seen upon substitution of amino acid residues that make either direct or water-mediated contacts with tRNA^{Gln} (*40*−*44*). In particular, the loop-strand-helix subdomain of GlnRS serves to physically connect the anticodon-binding and active-site domains (*44*, *45*). The β-strand of this subdomain in GlnRS was proposed to be structurally homologous to residues 354−359 of *E. coli* MetRS (*26*). To investigate whether a residue in this region of MetRS was important for domain−domain signaling, we replaced a highly conserved (in MetRS) Tyr357 with Phe and saw no significant effect on either tRNA or microhelix aminoacylation efficiency (data not shown). While further analysis of this region of the structure may be warranted, this result encouraged us to think in terms of a network of interactions between residues separated in space and not simply in a linker sequence. Thus, N387 and N452 were examples of residues that could be part of such a potential network that was essential for induced-fit-dependent generation of an active synthetase−tRNA complex.

We cannot rule out the possibility of a direct interaction between N387 and N452 with tRNA^{Met}. However, all previously described functional contacts between MetRS and tRNA^{Met} are localized to the anticodon and acceptor stem. They do not involve nucleotides outside of these regions. In the structure of glutaminyl-tRNA synthetase with tRNA^{Gln}, protein−tRNA contacts are also concentrated in the acceptor stem and anticodon (*25*). Because MetRS is related to GlnRS by virtue of both enzymes having the class I architecture, the GlnRS−tRNA^{Gln} complex was used to develop a model for the MetRS−tRNA^{Met} complex (*26*). In this model, neither N387 nor N452 is at the enzyme−tRNA interface. Thus, this model is consistent with our data showing that neither N387 nor N452 makes contact with the two major loci for tRNA contacts. For these reasons, we favor the idea that N387 and N452 are an important part of the induced-fit-based mechanism of generating the active conformation of bound tRNA^{Met}.

In the 2.5 Å crystal structure of *E. coli* MetRS (*12*), the carboxyl oxygen of Asn452 and the amine hydrogen of Asn387 are separated by 6.1 Å [we estimate that the corresponding distance in the newly solved *T. thermophilus* MetRS structure is comparable (*36*)]. If fixed, this spacing would rule out a direct (or water-mediated) hydrogen-bonding interaction between the two side chains. However, a small repositioning of either or both of these side chains could easily bring about a direct or water-mediated interaction. This repositioning could be induced by the bound tRNA and may be critical for the communication between the anticodon and the active site.

By way of possible analogy, the G10:U25 base pair in the D-stem of tRNA^{Asp} is important for aminoacylation efficiency (*46*). And yet, this base pair makes no direct contact with aspartyl-tRNA synthetase. Like N387 and N452 in MetRS, the G10:U25 pair of aspartyl-tRNA synthetase may be important for generating the active (and distorted) bound conformation (*47*).

Earlier we showed that the sum of the interaction free energies for association of the isolated arms of tRNA (microhelix and anticodon stem-loop) with MetRS is considerably more than needed to account for the free energy of binding of the native tRNA (*48*). The excess free energy from favorable acceptor helix and anticodon stem-loop contacts is thought to offset the cost of induced fit, where the tRNA structure is strained to create the active conformation for aminoacylation. [The distortion of the acceptor stem and anticodon of tRNA^{Gln} complex is another example in point (*25*).] The N387A/N452A substitutions do not affect interactions with the isolated anticodon stem-loop or microhelix. This observation suggests that the binding of these isolated components to MetRS is without the price of induced fit. Only when there is covalent continuity of the tRNA structure can its two domains bind simultaneously, and it is under those circumstances that the active conformation is associated with induced fit and distortion is generated.

A complete disruption of the communication between the anticodon and active site should reduce aminoacylation efficiency by several orders of magnitude. While the 30-fold decrease in anticodon-activated aminoacylation we observed with the N387A/N452A mutant enzyme is far below the reduction in efficiency one might expect for a complete loss of communication, a signaling pathway dependent on only a few side-chain interactions would presumably be disadvantageous to the enzyme. It is likely therefore that N387 and N452 are but two of several residues

in *E. coli* MetRS responsible for interdomain communication.

ACKNOWLEDGMENT

We thank Dr. Tyzoon Nhomanbhoy for assistance with fluorescence experiments and Dr. Lluís Ribas de Pouplana for helpful discussions.

REFERENCES

1. Webster, T., Tsai, H., Kula, M., Mackie, G. A., and Schimmel, P. (1984) *Science 226*, 1315−1317.
2. Eriani, G., Delarue, M., Poch, O., Gangloff, J., and Moras, D. (1990) *Nature 347*, 203−206.
3. Cusack, S., Berthet-Colominas, C., Hartlein, M., Nassar, N., and Leberman, R. (1990) *Nature 347*, 249−255.
4. Hountondji, C., Lederer, F., Dessen, P., and Blanquet, S. (1986) *Biochemistry 25*, 16−21.
5. Schimmel, P. (1987) *Annu. Rev. Biochem. 56*, 125−158.
6. Park, S. J., and Schimmel, P. (1988) *J. Biol. Chem. 263*, 16527−16530.
7. Dock-Bregeon, A. C., Garcia, A., Giegé, R., and Moras, D. (1990) *Eur. J. Biochem. 188*, 283−290.
8. Schulman, L. H., and Pelka, H. (1988) *Science 242*, 765−768.
9. Kim, H. Y., Pelka, H., Brunie, S., and Schulman, L. H. (1993) *Biochemistry 32*, 10506−10511.
10. Kim, S., Ribas de Pouplana, L., and Schimmel, P. (1994) *Biochemistry 33*, 11040−11045.
11. Auld, D. S., and Schimmel, P. (1995) *Science 267*, 1994−1996.
12. Brunie, S., Zelwer, C., and Risler, J. L. (1990) *J. Mol. Biol. 216*, 411−424.
13. Leon, O., and Schulman, L. H. (1987) *Biochemistry 26*, 5416−5422.
14. Ghosh, G., Pelka, H., and Schulman, L. H. (1990) *Biochemistry 29*, 2220−2225.
15. Meinnel, T., Mechulam, Y., Blanquet, S., and Fayat, G. (1991) *J. Mol. Biol. 220*, 205−208.
16. Muramatsu, T., Nishikawa, K., Nemoto, F., Kuchino, Y., Nishimura, S., Miyazawa, T., and Yokoyama, S. (1988) *Nature 336*, 179−181.
17. Meinnel, T., Mechulam, Y., Le Corre, D., Panvert, M., Blanquet, S., and Fayat, G. (1991) *Proc. Natl. Acad. Sci. U.S.A. 88*, 291−295.
18. Lee, C. P., Dyson, M. R., Mandal, N., Varshney, U., Bahramian, B., and RajBhandary, U. L. (1992) *Proc. Natl. Acad. Sci. U.S.A. 89*, 9262−9266.
19. Martinis, S. A., and Schimmel, P. (1992) *Proc. Natl. Acad. Sci. U.S.A. 89*, 65−69.
20. Martinis, S. A., and Schimmel, P. (1993) *J. Biol. Chem. 268*, 6069−6072.
21. Gale, A. J., and Schimmel, P. (1995) *Biochemistry 34*, 8896−8903.
22. Alexander, R. W., Nordin, B. E., and Schimmel, P. (1998) *Proc. Natl. Acad. Sci. U.S.A. 95*, 12214−12219.
23. Kim, S., and Schimmel, P. (1992) *J. Biol. Chem. 267*, 15563−15567.
24. Ribas de Pouplana, L., Auld, D. S., Kim, S., and Schimmel, P. (1996) *Biochemistry 35*, 8095−8102.
25. Rould, M. A., Perona, J. J., Söll, D., and Steitz, T. A. (1989) *Science 246*, 1135−1142.
26. Perona, J. J., Rould, M. A., Steitz, T. A., Risler, J. L., Zelwer, C., and Brunie, S. (1991) *Proc. Natl. Acad. Sci. U.S.A. 88*, 2903−2907.
27. Schmitt, E., Meinnel, T., Panvert, M., Mechulam, Y., and Blanquet, S. (1993) *J. Mol. Biol. 233*, 615−628.
28. Yanisch-Perron, C., Vieira, J., and Messing, J. (1985) *Gene 33*, 103−119.
29. Bradford, M. M. (1976) *Anal. Biochem. 72*, 248−254.
30. Seong, B. L., and RajBhandary, U. L. (1987) *Proc. Natl. Acad. Sci. U.S.A. 84*, 334−338.
31. Calendar, R., and Berg, P. (1966) *Biochemistry 5*, 1690−1695.
32. Blanquet, S., Iwatsubo, M., and Waller, J. P. (1973) *Eur. J. Biochem. 36*, 213−226.
33. Dardel, F., Panvert, M., and Fayat, G. (1990) *Mol. Gen. Genet. 223*, 121−133.
34. Cassio, D., and Waller, J. P. (1971) *Eur. J. Biochem. 20*, 283−300.
35. Mellot, P., Mechulam, Y., Le Corre, D., Blanquet, S., and Fayat, G. (1989) *J. Mol. Biol. 208*, 429−443.
36. Sugiura, I., Nureki, O., Ugaji, Y., Kuwabara, S., Shimada, A., Tateno, M., Lorer, B., Giegé, R., Moras, D., Yokoyama, S., and Konno, M. (1999) PDB accession number 1A8H.
37. Ghosh, G., Pelka, H., Schulman, L. H., and Brunie, S. (1991) *Biochemistry 30*, 9569−9575.
38. Rould, M. A., Perona, J. J., and Steitz, T. A. (1991) *Nature 352*, 213-218.
39. Jahn, M., Rogers, M. J., and Söll, D. (1991) *Nature 352*, 258−260.
40. Rogers, M. J., Adachi, T., Inokuchi, H., and Söll, D. (1994) *Proc. Natl. Acad. Sci. U.S.A. 91*, 291−295.
41. Weygand-Duraševic, I., Rogers, M. J., and Söll, D. (1994) *J. Mol. Biol. 240*, 111−118.
42. Ibba, M., Hong, K. W., Sherman, J. M., Sever, S., and Söll, D. (1996) *Proc. Natl. Acad. Sci. U.S.A. 93*, 6953−6958.
43. Kitabatake, M., Ibba, M., Hong, K. W., Söll, D., and Inokuchi, H. (1996) *Mol. Gen. Genet. 252*, 717−722.
44. Sherman, J. M., Thomann, H. U., and Söll, D. (1996) *J. Mol. Biol. 256*, 818−828.
45. Perona, J. J., Rould, M. A., and Steitz, T. A. (1993) *Biochemistry 32*, 8758−8771.
46. Pütz, J., Puglisi, J. D., Florentz, C., and Giegé, R. (1991) *Science 252*, 1696−1699.
47. Ruff, M., Krishnaswamy, S., Boeglin, M., Poterszman, A., Mitschler, A., Podjarny, A., Rees, B., Thierry, J. C., and Moras, D. (1991) *Science 252*, 1682−1689.
48. Gale, A. J., Shi, J. P., and Schimmel, P. (1996) *Biochemistry 35*, 608−615.

BI991948C